

BILJANA ANGIJUSHEVA
EMILIJA FIDANCEVSKA
VOJO JOVANOVIĆ

Faculty of Technology and Metallurgy,
University "Ss. Cyril and Methodius",
Skopje,
Republic of Macedonia

SCIENTIFIC PAPER

UDC 666.3/.7(497.17):666.3–187

DOI 10.2298/CICEQ110607001A

PRODUCTION OF CERAMICS FROM COAL FLY ASH

Dense ceramics are produced from fly ash from REK Bitola, Republic of Macedonia. Four types of fly ash from electrofilters and one from the collected zone with particles <0.063 mm were the subject of this research. Consolidation was achieved by pressing ($p = 133$ MPa) and sintering (950, 1000, 1050 and 1100 °C and heating rates of 3 and 10 °C/min). Densification was realized by liquid phase sintering and solid state reaction where diopside $[Ca(Mg,Al)(Si,Al)_2O_6]$ was formed. Ceramics with optimal properties (porosity $2.96 \pm 0.5\%$, bending strength 47 ± 2 MPa, compressive strength 170 ± 5 MPa) was produced at 1100 °C using a heating rate of 10 °C/min.

Keywords: fly ash, ceramics, sintering, bending strength, compressive strength.

In the last decade there has been a growing interest for solving problems related to environmental pollution with industrial wastes. One such example is industrial waste from the coal combustion process in thermal power plants. The total quantity of coal combustion by-products in Europe for 2008 is 56 million tons [1]. The highest percent (around 66.6%) belongs to fly ash but the quantity that is utilized exceeds no more than 17 million tons. The highest utilization of coal fly ash is in the construction industry as a concrete addition or a replacement for part of the cement [2-5], then road base construction [6,7], landfill liners [8-10], and agriculture [11,12]. However, new applications and possibilities for utilization of coal fly ash are needed. Fly ash is a by-product of the burning of coal between the temperature range of 1100 and 1450 °C, and contains valuable oxides, such as SiO_2 , Al_2O_3 , CaO , Fe_2O_3 and other oxides provided as powder with fine particles [13]. There has been considerable research on the production of ceramics from coal fly ash with the addition of the natural raw materials or waste materials [14-16].

Fukumoto *et al.* [17] explored the suitability of using fly ash and clay in order to produce composite material with satisfactory mechanical properties. Re-

searchers have investigated the influence of the sintering procedure on the mixture of fly ash, with a changing ratio of clay 0-10% on the mechanical properties of the composite materials. They have emphasized the reinforcement role of coal ash particles to clay base material during the electric furnace burning. For spark plasma sintering, clay plays the role of a binder effect due to liquid phase sintering by clay melting.

There are several reports for producing a porous structure from fly ashes and different additives [18-20]. Zimmer *et al.* [21] utilized in their studies traditional raw materials, such clay, limestone, feldspar and fly ash, in order to produce ceramic materials with satisfactory technological properties, allowing the production of ceramic tiles.

There are fewer works that deal with the topic of receiving the ceramics from pure fly ash. Pimraksa *et al.* [22] used pure fly ash for the production of bricks. They studied the influence of treatments such as sieving and grinding on the properties of the sintered ceramics.

The aim of this paper is to describe the production of dense ceramics obtained from five zones of electrofilter (fraction <0.063 mm). The consolidation of the fly ashes was applied in order to produce ceramics with minimum porosity, homogeneous microstructure and high mechanical properties by varying the process parameters, i.e. the sintering temperature and heating rate.

Corresponding author: B. Angjusheva, Faculty of Technology and Metallurgy, University "Ss. Cyril and Methodius", Rudjer Bošković 16, Skopje, Republic of Macedonia.

E-mail: angjushevab@yahoo.com

Paper received: 7 June, 2011

Paper revised: 17 November, 2011

Paper accepted: 3 January, 2012

MATERIALS AND METHODS

Characterization of the fly ash

Fly ash from the thermal power plant REK Bitola, Republic of Macedonia, was used as raw material for producing ceramics. Four fly ash samples with lignite origin from different zones of electrofilter, coded as FA1, FA2, FA3 and FA4 and from the collected zone coded as CZ, were the subject of this study.

The morphology of the received fly ashes was followed by scanning electron microscope (Leica S 440I) and the particle size distribution was determined by sieving analyses (Retsch AS200). Further investigation was conducted on the fly ashes with a fraction lower than 0.063 mm.

Chemical analysis of the fly ashes was carried out by X-ray fluorescence (ARL 990XP). Unburnt carbon content was determined from the loss of ignition (LOI) on a dried sample heated at 900 °C for 2 h at maximum temperature. The phase composition of the fly ashes was performed by using X-ray diffraction (Philips, model PV 105-1) operating at $\text{CuK}\alpha$ radiation at an accelerating voltage of 40 kV and a current of 40 mA. The Pycnometer method was applied for the purpose of determining the specific gravity. In order to determine the specific surface area of the fly ashes, the BET method (Micromeritics, Gemini) was applied. The thermal properties of the fly ashes were determined using a heating microscope (Leitz Wetzlar) in the temperature interval from room temperature (RT) to 1400 °C, in air atmosphere with a heating rate of 10 °C/min.

Consolidation of the fly ash samples

The fly ash particles with dimensions lower than 0.063 mm were granulated using a certain amount of water from 17 to 20 wt.%, gradually drop-wise into fly ash. The moistened fly ash was granulated through a 0.6 mm sieve. Pressing of the granulated fly ash was performed by uniaxial press (Weber Pressen KIP 100) at $p = 133$ MPa. Green density was calculated from the weight to volume ratio of unfired samples.

Fly ash samples were sintered in the chamber furnace in air atmosphere at temperatures of 950, 1000, 1050 and 1100 °C with a holding time at a maximum temperature of 60 min. The applied heating rates for sintering were 3 and 10 °C/min, while the cooling of the samples was not controlled.

Characterization of the sintered samples

Bulk density was calculated from the weight to volume ratio of the sintered samples. Sample shrinkage (%) was measured from the differences in the green and fired samples' length. Water absorption of

the sintered samples was determined from the difference between dry mass, m_{dry} , and surface dry mass, $m_{\text{sur.dry}}$, after immersion in cold water. Porosity of the samples was calculated from the relative density.

The microstructure of the sintered fly ash samples was examined by means of scanning electron microscopy (Leica S440I). The samples were coated with gold prior to examination.

The bending strength was measured on the sintered samples (with the dimensions of 50 mm×5 mm×5 mm), which were subjected to a 3-point bending strength tester (Netzsch 401/3) with a 30 mm span and a 0.5 mm/min loading rate. The compressive strength tests were carried out using an Instron testing machine (model 1126) with a crosshead speed of 0.5 mm/min. For these mechanical tests at least five samples were used per each mentioned type, and the results were averaged.

Linear thermal expansion of the dense compacts was determined using the dilatometer (Netzsch 402E) in the air atmosphere and temperature interval RT-650 °C-RT, with a heating rate of 2 °C/min.

RESULTS AND DISCUSSION

Morphology of the received fly ashes

The morphology of the received fly ashes (CZ and FA1-FA4) are presented in Figure 1.

The typical morphology of fly ash powders can be seen from the SEM micrographs in Figure 1. Spherical particles with a broad particle size distribution, the porous sphere and particles with irregular geometry and dimensions are evident. The particles in CZ have the most heterogenic distribution and the dimensions varied from 10 to 200 μm , as seen in Figure 1a. A more uniform geometry and more spherical particles are present in the ashes starting from FA1 up to FA4. Namely, the dimensions of the particles varied for FA1 from 5 to 100 μm , in Figure 1b, for FA2 from 2 to 50 μm , in Figure 1c, for FA3 from 2 to 20 μm , in Figure 1d, and for FA4 from 1 to 10 μm , in Figure 1e. In addition, the size of agglomerates differs in fly ash powders and the degree of agglomeration is related to the particles' size. The highest agglomeration is present in FA4, Figure 1e, due to the presence of the smallest particle.

Particle size distribution of received fly ashes

The particle size distribution of the fly ashes is given in Table 1.

It is evident from Table 1 that in all fly ashes the fraction 0.063 mm is the most dominant. Namely, the quantity of 0.063 mm per fraction in CZ is 43.60 wt.%, but the quantity of the same fraction in FA4 is doubled

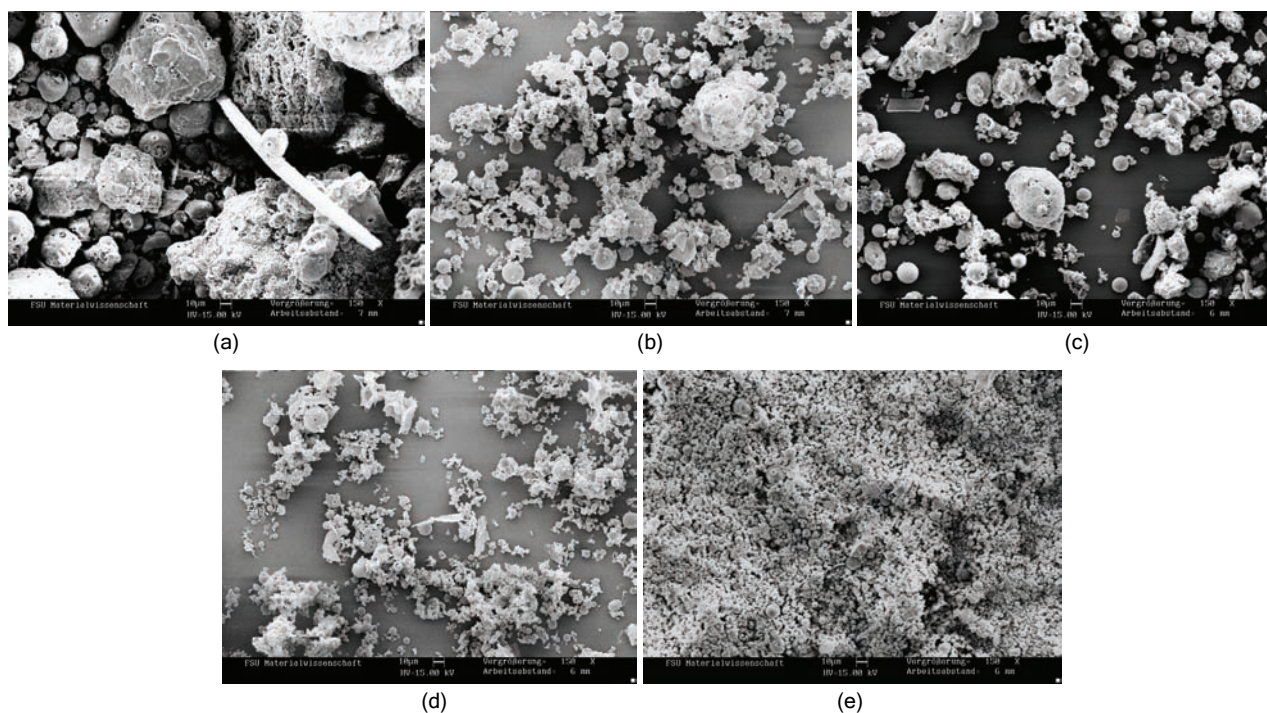


Figure 1. SEM Micrographs of the investigated fly ashes: a - CZ, b - FA1, c - FA2, d - FA3 and e - FA4 (bar 10 μm).

(82.36 wt.%), so the FA4 is the finest fly ash. The low content of the coarse fractions (larger than 0.250 mm) is evident in all fly ashes. The content of the coarse fraction for the CZ is 11.9 wt.% and subsequently decreases for the rest of the fly ashes reaching the value of 0.24 wt.% for FA4. The medium fraction (0.250–0.125 mm) in CZ is 43.80 wt.% and it is almost the same as the content of the fine fraction. The content of the medium fraction for the fly ashes FA1 to FA4 decreases and the lowest content is evident in FA4 (16.9 wt.%).

Table 1. Particle size analysis of the fly ash

Diameter, mm	Content, wt. %				
	CZ	FA1	FA2	FA3	FA4
+ 1.0	0.6	0.5	0.4	-	-
- 1.0 + 0.5	2.20	1.40	0.80	0.05	0.04
- 0.5 + 0.25	9.10	6.60	2.20	0.40	0.20
- 0.25 + 0.125	18.90	18.90	12.60	3.70	2.20
- 0.125 + 0.063	24.90	23.60	26.80	18.1	14.70
- 0.063 + 0.045	43.60	48.60	56.60	77.6	82.36
Σ	99.3	99.6	99.4	99.85	99.5

As the fraction less than 0.063 mm is the most reactive part of fly ashes, it was used as a starting point material for the next investigations for all types of the received fly ashes.

Chemical and physical properties of the fly ashes

Chemical composition and loss of ignition

The chemical composition of the investigated fly ashes (a fraction less than 0.063 mm) is given in Table 2.

Table 2. Chemical composition of the fly ashes

Oxide	Content, wt. %				
	CZ	FA1	FA2	FA3	FA4
SiO ₂	50.33	53.31	49.20	48.81	49.51
Al ₂ O ₃	18.59	19.92	18.78	17.81	17.62
Fe ₂ O ₃	7.71	7.68	7.72	7.80	7.91
CaO	13.76	10.74	13.23	14.31	13.77
MgO	3.05	2.70	3.04	3.39	3.36
Na ₂ O	1.07	0.84	0.78	0.70	0.69
K ₂ O	1.41	1.51	1.45	1.38	1.46
SO ₃	1.44	1.03	1.78	2.76	3.52
LOI	2.60	2.20	2.03	1.78	1.57
Σ	99.96	99.93	98.01	98.74	99.41

It is evident from Table 2 that the major chemical components in the fly ashes are: SiO₂, Al₂O₃ and CaO. In all the fly ashes, the content of CaO is higher than 10% and can be characterized as Class C fly ashes. According to ASTM C618 [23] fly ashes from lignite coals have a relatively large content of CaO and they are classified as Class C ashes.

Free CaO was not detected in the investigated fly ashes. According to Kiattikomol *et al.* [24] the pozzolanic activity of the fly ash is influenced by calcium in the glass, and not by the free calcium oxide nor crystalline CaO.

The content of LOI slightly decreased, starting from CZ (2.60 wt.%) towards FA4 (1.57 wt.%). The values of LOI are related to the existence of the unburnt coal particles, and according to Itskos *et al.* [25] it is also a result of the thermal disruption of some of its components.

Phase composition

From the XRD patterns of the CZ and FA4 presented in Figure 2, the presence of the principal crystalline phases is obvious: SiO₂ - quartz, CaAl₂Si₂O₈ - anorthite, Fe₂O₃ - hematite, NaAlSi₃O₈ - albite, CaSO₄ - anhydrite and an amorphous phase. In addition, the presence of quartz and anorthite are more emphasized in the CZ compared to FA4. The detected anhydrite is a characteristic phase in class C fly ashes. Gikunoo [26] reports that for most of the ashes, only about half of the SO₃ occurred as anhydrite while the rest play a role in the formation of alkali sulphates.

From the intensity of the peaks it is obvious that anhydrite is more present in FA4. This is in relation to the SO₃ content detected from the chemical analysis in Table 2. Namely, the SO₃ content in CZ is 1.44 wt.%, but the amount of SO₃ in FA4 is more than double (3.52 wt.%). The existence of anhydrite in the finer fractions of the ashes is confirmed in the literature as well [25]. From the XRD patterns it is as well obvious that there is a significant difference in the amorphous phase present in the FA4 compared to CZ, which is reflected in the high reactivity of FA4 compared to CZ. According to [27] the glass fraction in fly ashes usually varies between 70 and 89% depending on the type and coal source, degree of pulverisation, combustion conditions in the furnace, and the cooling rate of the combustion residue.

Specific surface area and specific gravity of the fly ashes and green density of the compacts

Table 3 presents the specific gravity, surface area of the fly ashes and green density of the compacts.

The specific gravity of fly ashes is in the range between 2.28 and 2.42 g/cm³. It is reported [26] that

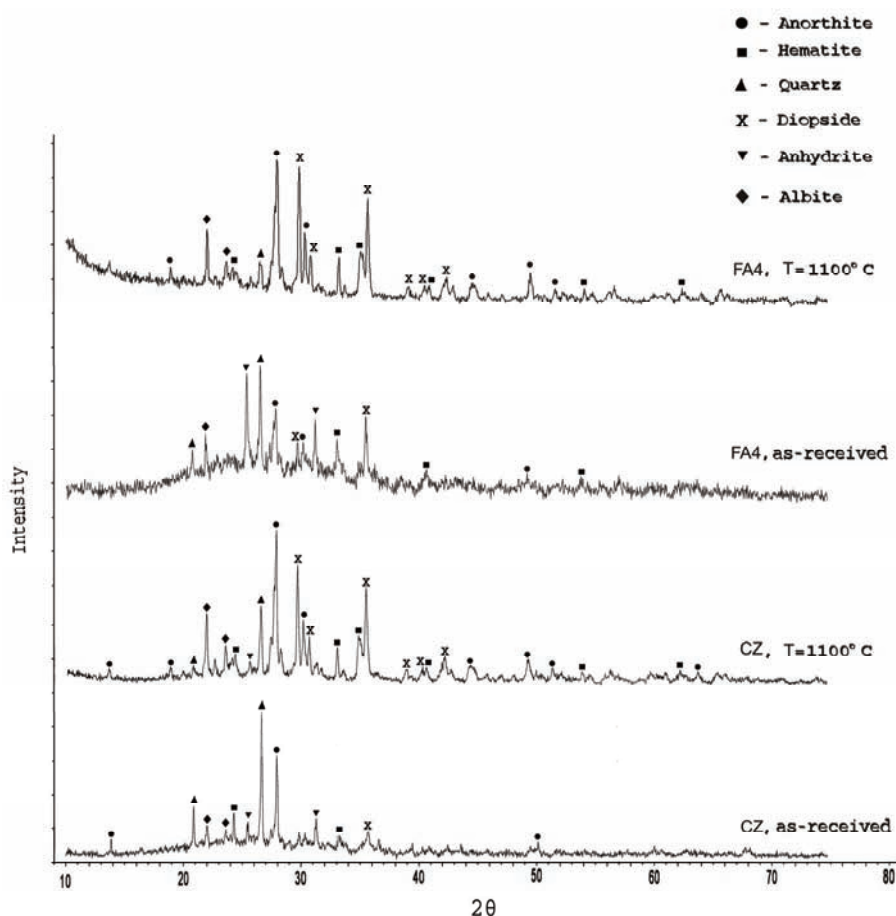


Figure 2. XRD Data for CZ and FA4 - as received, and CZ and FA4 sintered at 1100 °C $dT/dt = 10$ °C/min.

the specific gravity of fly ash generally varies from 1.3 to 4.8 g/cm³ and it is closely related to the shape and chemical composition of fly ash particles.

Table 3. Specific gravity, specific surface area of the fly ashes and green densities of the compacts

Property	CZ	FA1	FA2	FA3	FA4
Specific gravity, g/cm ³	2.28	2.27	2.32	2.38	2.42
Specific surface area, m ² /g	3.09	3.68	4.99	6.10	11.31
Green density, g/cm ³	1.524	1.519	1.520	1.524	1.556

The specific surface area increased from FA1 to FA4 reaching the value of 11.31 m²/g and it is almost 3.5 times higher than the value of the CZ. The differences are due to the different size, form and relief of the particles.

Concerning the green density, FA4 showed the highest density which is a result of the better packing of the particles during the pressing as a consequence of the high amount of fine particles present in FA4. Higher green density promotes a greater density of the sintered compacts [29].

Thermal properties of the fly ashes

The thermal properties of the fly ashes are given in Table 4.

Table 4. Thermal properties of the investigated fly ashes

Sample	Significant shrinkage, °C	Softening temperature, °C	Melting temperature, °C	Sintering region, °C
CZ	1190±10	1240±10	1300±10	1190-1240±10
FA1	1194±10	1250±10	1320±10	1194-1250±10
FA2	1200±10	1246±10	1310±10	1200-1246±10
FA3	1180±10	1200±10	1270±10	1180-1200±10
FA4	1110±10	1220±10	1240±10	1110-1220±10

According to the data presented in Table 4, it is evident that all types of fly ashes have a narrow region of sintering (1190-1250)±10 °C, except for FA4 (1110-1220)±10 °C. The melting temperature for CZ is 1300±10 °C, while for the rest of the fly ashes, they are in the interval from (1270-1320)±10 °C, and for FA4, it is 1240±10 °C.

Physical and thermal properties of sintered samples

The variation of density, porosity, water absorption and linear shrinkage with a temperature at a heating rate of 3 and 10 °C/min are presented in Figures 3-6.

The densities of the all FA compacts in the sintering region from 950 to 1050 °C for both heating rates are close, *i.e.*, in the ranges from 1.50±0.02 to 1.61±0.02 g/cm³ (Figures 3a and 3b). For all the fly ash compacts, the density at a temperature of 1100 °C increased for both the applied heating rates, particularly for FA4. One of the reasons for the highest density of FA4 (2.35±0.02 g/cm³) is a lower content of residual coal and as a consequence during the sintering the lower porosity has been produced. The particle with no defined geometry influenced the package of the powders. Thus, the smaller the particle size, the smaller the space (pores) among the particles that is generated during the package of the powders, and in

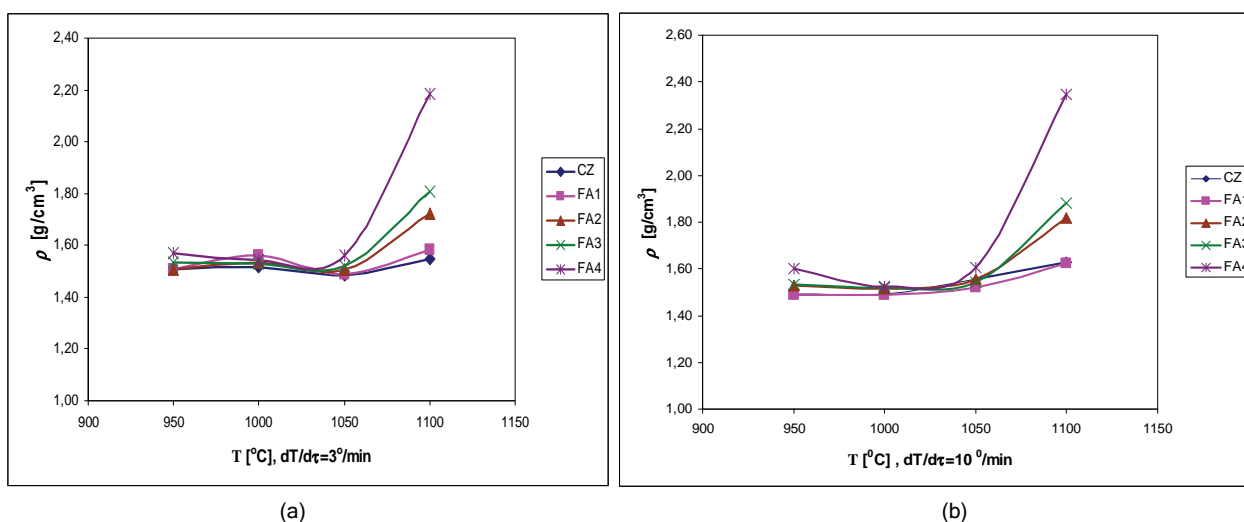


Figure 3. Density of sintered fly ash compacts using heating rate: a - 3 and b - 10 °C/min.

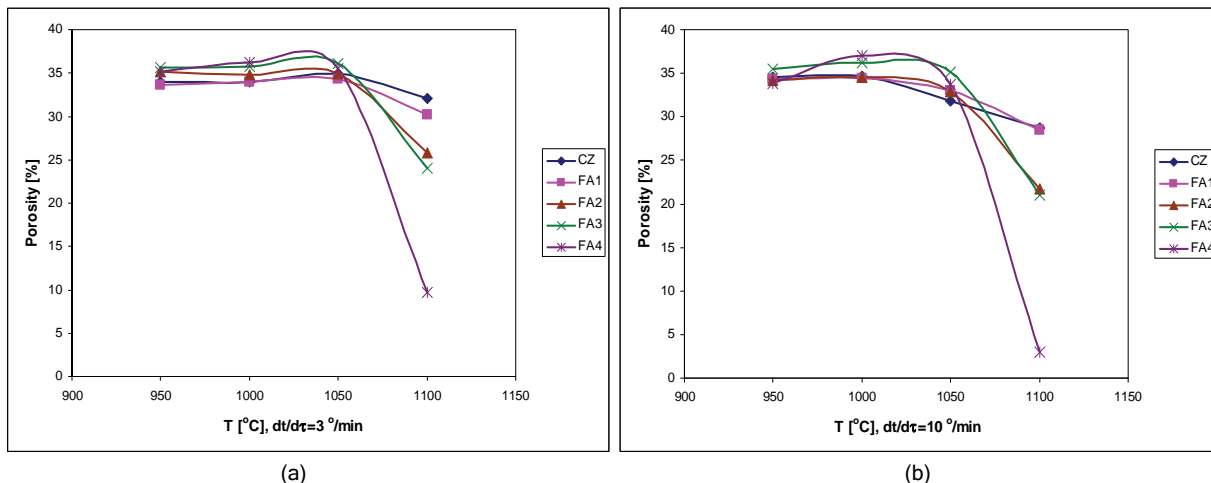


Figure 4. Porosity of the sintered fly ash compacts using heating rate: a - 3 and b - 10 $^{\circ}\text{C}/\text{min}$.

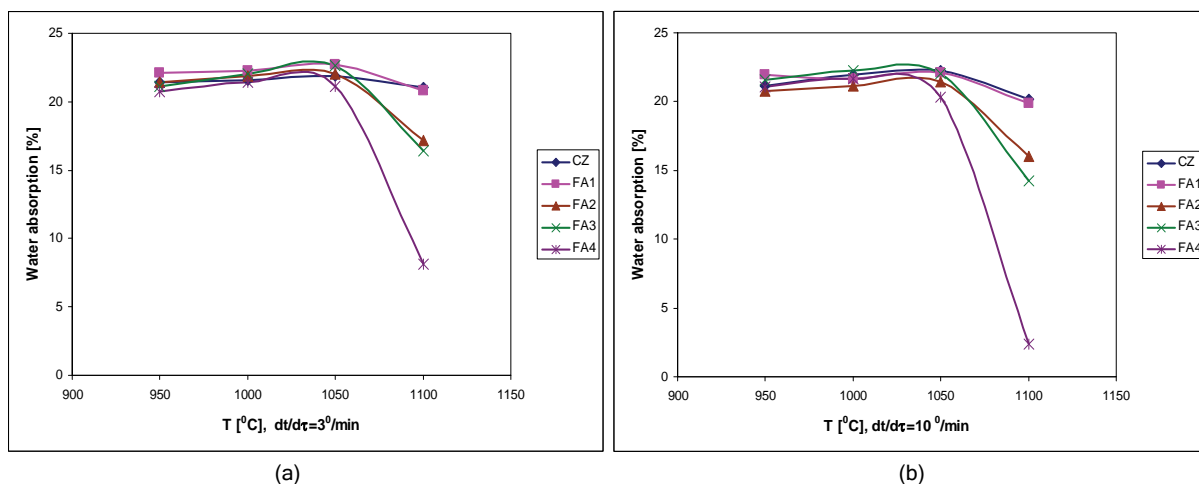


Figure 5. Water absorption of the sintered fly ash compacts using heating rate: a - 3 and b - 10 $^{\circ}\text{C}/\text{min}$.

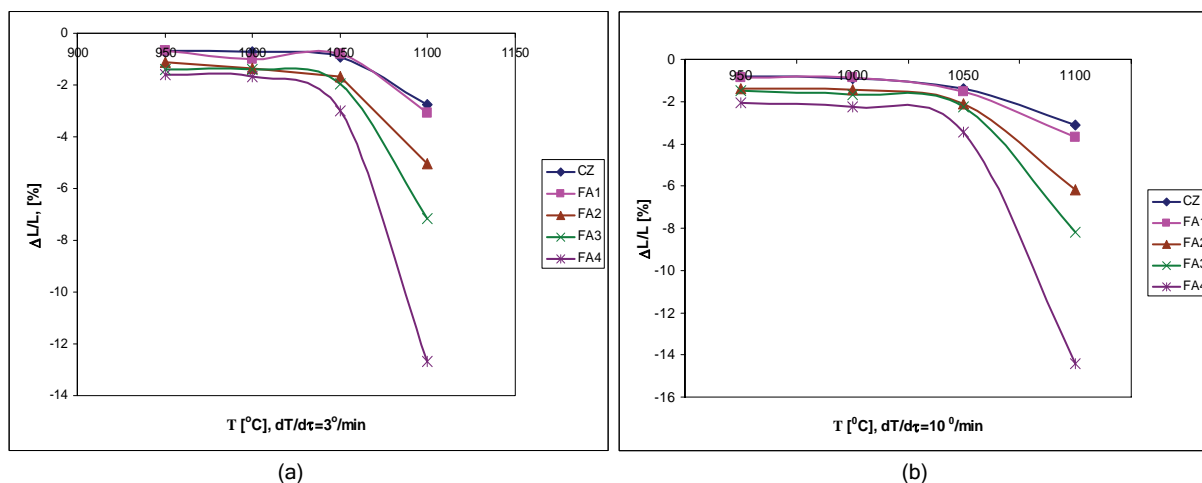


Figure 6. Shrinkage of sintered fly ash compacts using heating rate: a - 3 and b - 10 $^{\circ}\text{C}/\text{min}$.

the course of sintering the smaller pores are easily eliminated and the compacts with lower porosity are produced [29].

Concerning the differences of the heating rates using the heating rate of 3 $^{\circ}\text{C}/\text{min}$, the density was $2.18 \pm 0.02 \text{ g}/\text{cm}^3$, but for the heating rate of 10 $^{\circ}\text{C}/\text{min}$,

the density of $2.35 \pm 0.02 \text{ g/cm}^3$ was achieved, which is in accordance with the literature [30].

From Figure 4 it is evident that the porosity of the all fly ash samples decrease at a temperature of $1100 \text{ }^\circ\text{C}$, and it is the most expressed for FA4. Thus, the porosity for CZ, sintered at $1100 \text{ }^\circ\text{C}$ using a heating rate of $10 \text{ }^\circ\text{C/min}$, was $28.5 \pm 2\%$, while the porosity for FA4 samples, sintered under the same conditions, was $2.96 \pm 0.5\%$.

The data for water absorption presented in Figure 5 shows that the FA4 has the lowest value (2.39 wt.%) at a temperature of $1100 \text{ }^\circ\text{C}$, using a heating rate of $10 \text{ }^\circ\text{C/min}$. The values for density, water absorption and porosity are better than the values reported by Ilic *et al.* [31] and Pimraksa *et al.* [22].

The maximal shrinkage has the sample FA4 (13 wt.%) and according to [32] it is a result of the high reactivity, *i.e.*, the higher factor of geometrical activity.

The characteristic of thermal expansion determined in the interval of RT– $650 \text{ }^\circ\text{C}$ –RT showed absence of hysteresis, which proves that the obtained ceramic compacts are in thermal equilibrium [19]. The technical coefficient for CZ and FA4, sintered at $1100 \text{ }^\circ\text{C}$ using the heating rate of $10 \text{ }^\circ\text{C/min}$, is 8.30 and $8.58 \times 10^{-6}/^\circ\text{C}$, respectively, and corresponds to the value reported in literature [33].

Mechanical properties of the sintered samples

In Figure 7, the bending strength of the fly ash compacts *versus* the sintering temperature for both the heating rates are presented.

Generally, for all FA compacts, by increasing the temperature up to $1050 \text{ }^\circ\text{C}$ the bending strength is also increased and there are no significant differences in bending strengths, no matter if the heating rate was 3 or $10 \text{ }^\circ\text{C/min}$. The significant difference of

bending strength is evident at higher sintering temperatures. The FA4 compacts showed the highest values of bending strength for the investigated sintering region. Namely, the bending strength for FA4 at $950 \text{ }^\circ\text{C}$ was $14.26 \pm 1 \text{ MPa}$, but at the final temperature of $1100 \text{ }^\circ\text{C}$ the maximum bending strength of $47.01 \pm 2 \text{ MPa}$ was reached. The highest values of the bending strength of FA4 compacts is directly related to the lower residual coal content, narrow particle size distribution and the morphology of the fly ash particles. As a consequence the compacts with high density/lower porosity and high mechanical properties were obtained. The bending strength for CZ compacts was the lowest for the whole investigated temperature region, starting from $6 \pm 1 \text{ MPa}$ at $950 \text{ }^\circ\text{C}$ up to $16.5 \pm 1 \text{ MPa}$ at $1100 \text{ }^\circ\text{C}$.

Further research was conducted only to the FA4 and CZ compacts, as the most favorable investigated systems due to the highest physical and mechanical properties - FA4, and the integral quantity of CZ produced during the combustion of coal.

Figure 8 presents the variation of the compressive strength of CZ and FA4 compacts with the sintering temperature for both the heating rates.

It is evident that for the FA4 the compressive strength increased from 70 ± 3 to $170 \pm 5 \text{ MPa}$ by increasing the sintering temperature from 950 to $1100 \text{ }^\circ\text{C}$ using the heating rate of $10 \text{ }^\circ\text{C/min}$. The bending and compressive strength for the sintered FA4 compacts are higher than those reported by Pimraksa *et al.* [22] for the investigated temperature region.

It is obvious that the mechanical properties of the investigated fly ash compacts have generally higher values when the heating rate of $10 \text{ }^\circ\text{C/min}$ was used during the sintering. It can be explained that one of the reasons is limiting the oxygen access to the

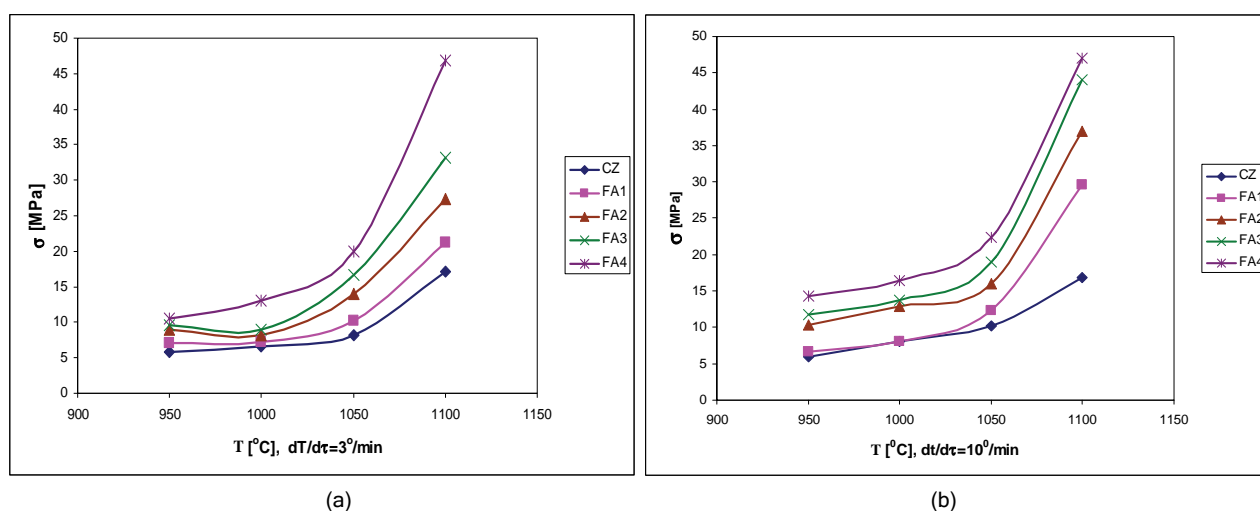


Figure 7. Bending strength of the fly ash compact sintered at different temperature using heating rate: a - 3 and b - $10 \text{ }^\circ\text{C/min}$.

carbon in the compact interior described in [34]. Applying the higher heating rate during the sintering, the surface of the compact is sintered and becomes virtually impervious to air. As a result, the carbon particles encapsulated inside the specimen were not oxidized and did not generate any pores.

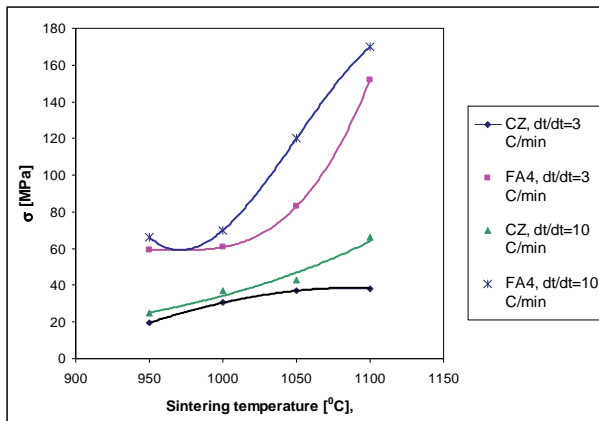


Figure 8. Plot of compressive strength of the samples in relation to sintering temperature.

XRD Studies of the sintered samples

The XRD patterns for received CZ and FA4 and sintered compacts of CZ and FA4 at a temperature of 1100 °C with a heating rate of 10 °C/min, are shown in Figure 2.

The crystalline phases in received CZ and FA4 are: quartz, anorthite, hematite and albite, and they remain (the same) in the sintered samples of CZ and FA4. Sintering the samples of CZ and FA4 at 1100 °C reduce the peaks of quartz (SiO_2) and anhydrite (CaSO_4) and are in accordance with [25]. On the other hand, sintering promotes the anorthite peaks ($\text{CaAl}_2\text{Si}_2\text{O}_8$). The relatively high content of CaO present in the received fly ashes is the reason for the formation of anorthite. As reported by Erol *et al.* [35], the substitution of the Ca ion into the SiO_2 - Al_2O_3 couple lead to the occurrence of anorthite at high temperatures. In addition, the new crystalline phase of diopside [$\text{Ca}(\text{Mg},\text{Al})(\text{Si},\text{Al})_2\text{O}_6$] was detected and the formation of diopside should be forced [36], because it generally displayed better physical properties due to the interlocking microstructure of its crystals.

The amorphous phase especially present in FA4 has been reduced during the sintering of the compacts.

Microstructural analysis

The microstructures of the fractured surface of the compacts CZ and FA4 sintered at 1100 °C with a heating rate of 10 °C/min are presented in Figures 9 and 10, respectively.

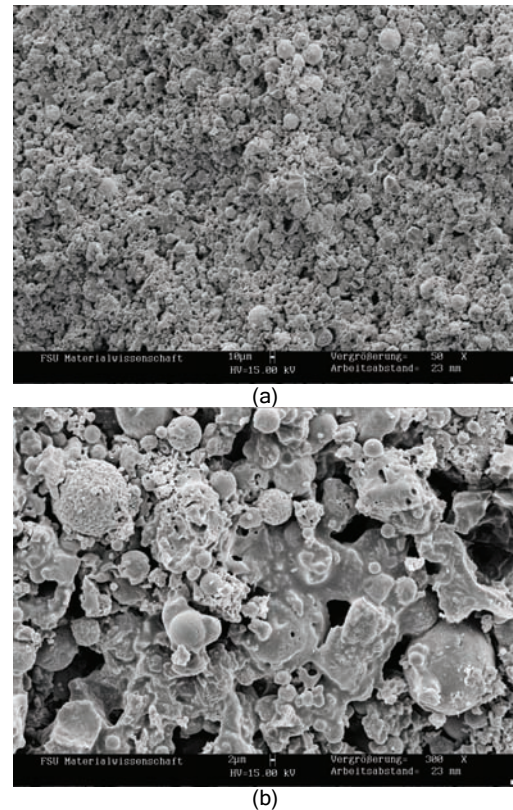


Figure 9. SEM Images for CZ, $T = 1100\text{ }^\circ\text{C}/1\text{h}$, $dT/dt = 10\text{ }^\circ\text{C}/\text{min}$; bars: a) 10 and b) 2 μm .

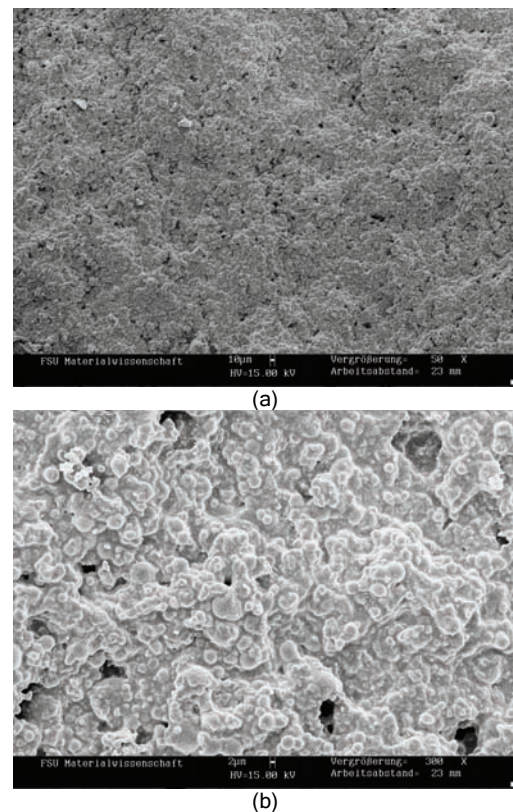


Figure 10. SEM Images for FA4, $T = 1100\text{ }^\circ\text{C}/1\text{h}$, $dT/dt = 10\text{ }^\circ\text{C}/\text{min}$; bars: a) 10 and b) 2 μm .

The microstructure of CZ compacts, Figures 9a and 9b, is heterogeneous with evident presence of liquid bridges among the grains. The dimension of the grains varied in a wide interval (from 5 to 70 μm). The biggest part of the spherical grains has kept their individuality and their dimensions are in the interval from 8 to 15 μm . The presences of the porous grains (10-20 μm) are also evident. The dimensions of intergranular pores are 2 ± 1 μm .

Figures 10a and 10b show the microstructure of the FA4 which is more homogeneous and smoother compared to the microstructure of CZ sintered at the same temperature. A significant presence of the liquid phase is evident through the whole surface of the sintered compact. There are also closed pores with dimensions no larger than 10 μm . One of the basic reasons for better densification of the FA4 compacts is the morphology of the particles. The different form of the particles and their smaller dimensions are the reasons for more frequent contacts among the particles. The narrow particle size distribution of FA4 is also the reason for interparticle neck formation and appearance of liquid phase at lower sintering temperatures, as reported in literature [29].

CONCLUSIONS

- Fly ash from the thermal power plant REK Bitola, Republic of Macedonia, was used for production of dense ceramics.

- The process variables of the sintering were: temperature in the interval between 950 and 1100 $^{\circ}\text{C}$, and a heating rate of 3 and 10 $^{\circ}\text{C}/\text{min}$. Four different fly ashes from different zones of electro filter (FA1 and FA4) and one from the collected zone (CZ) with a granulation of <0.063 mm were the subject of this research.

- Ceramics with a porosity of $2.96\pm 0.5\%$, density (2.35 ± 0.02 g/cm^3), bending strength 47.01 ± 2 MPa and compressive strength 170 ± 5 MPa, were produced at $p = 133$ MPa and $T = 1100$ $^{\circ}\text{C}$, using a heating rate of 10 $^{\circ}\text{C}/\text{min}$.

- Sintering in the presence of the liquid phase was evident at a temperature of 1100 $^{\circ}\text{C}$, but also the reaction of sintering among the CaO, SiO₂ and Al₂O₃ has resulted in the formation of diopside [Ca(Mg,Al)(Si,Al)₂O₆].

- The produced dense ceramics are the potential materials in the construction industry.

REFERENCES

- [1] European Coal Combustion Products Association e.V., <http://www.ecoba.com> (accessed 25 February 2011)
- [2] O.E. Manz, *Fuel* **76**(8) (1997) 691-696
- [3] L.K.A. Sear, International ash Symposium, Center for applied Energy Research, University of Kentucky, Paper 36 (2001)
- [4] J. Monzo, J. Paya, E. Peris-Mora, *Cem. Con. Res.* **24** (1994) 791-796
- [5] K.S. Wang, K.L. Lin, Z.Q. Huang, *Cem. Con. Res.* **31** (2001) 97-103
- [6] B.M. Galloway, Proceedings of the Fly Ash Applications in 1980 Conference, College Station, Texas (1980)
- [7] A. Mistra, S. Upadhyaya, D. Biswas, International Ash Utilization Symposium, Center for applied Energy Research, University of Kentucky, Paper 118 (2003)
- [8] J. Zerbe, J. Siepak, H. Elbanowska, *Pol. J. Environ. Stud.* **10**(2) (2001) 113-117
- [9] E. Çokça, J. Geotec. Geoenviron. Eng. **27**(7) (2001) 568-573
- [10] S.R. Kaniraj, V. Gayathri, *J. Ener. Eng.* **30**(1) (2004) 18-43
- [11] C. Heidrich, International Ash Utilization Symposium, Center for applied Energy Research, University of Kentucky, 2005
- [12] V. Kumar, K.A. Zacharia, G. Goswami, Fly Ash in Agriculture: Issues & Concerns, <http://www.tiffac.org.in/news/flyagr.htm> (accessed 25 February 2011)
- [13] R.D. Rawlings, J.P. Wu, A.R. Boccaccini, *J. Mater. Sci.* **41** (2006) 733-761
- [14] M.R. Little, V. Adell, A.R. Boccaccini, C.R. Cheeseman, *Res. Con. Rec.* **52**(11) (2008) 1329-1335
- [15] R. Rekecki, J. Ranogajec, *Proc. App. Ceram.* **2**(2) (2008) 89-95.
- [16] C.Y. Park, S.D. Yoon, Y.H. Yun, *J. Ceram. Proc. Res.* **8**(6) (2007) 435-439
- [17] I. Fukumoto, Y. Kanda, *J. Sol. Mech. Mat. Eng.* **3**(5) (2009) 739-747
- [18] J.P. Wu, A.R. Boccaccini, P.D. Lee, M.J. Kershaw, R.D. Rawlings, *Adv. App. Ceram.* **105**(1) (2006) 32-39
- [19] J. Bossert, E. Fidancevska, B. Mangutova, B. Panova, D. Milosevski, M. Milosevski, *Sci. Sin.* **36** (2004) 87-92
- [20] B. Mangutova, E. Fidancevska, M. Milosevski, J. Bossert, *APTEFF* **35** (2004) 103-110
- [21] A. Zimmer, C.P. Bergman, *Was. Manag.* **27**(1) (2007) 59-68
- [22] K. Pimraksa, M. Wilhelm, M. Kochberger, W. Wruss, International ash Symposium, Center for applied Energy Research, University of Kentucky, Paper 84 (2001).
- [23] Annual Book of ASTM Standards, B618-03, pp.459-467
- [24] K. Kiattikomol, C. Jataurpitakkul, S. Songpiriyakij, S. Chuttim, *Cem. Con. Comp.* **23** (2001) 335-343
- [25] G. Itskos, S. Itskos, N. Koukouzas, *Fuel Proc. Tech.* **91** (2010) 1558-1563
- [26] E. Gikunoo, Master thesis, University of Saskatchewan, Canada, 2004
- [27] S. Ghosal, J. L. Ebert and S. A. Self, *Fuel Proc. Tech.* **44** (1995) 81-94

- [28] A. Medina, P. Camero, X. Querol, N. Moreno, B. de Leon, M. Almanza, G. Vargas, M. Izquierdo, O. Font, J. Haz. Mater. **181** (2010) 82-90
- [29] E. Benavidez, C. Grasselli, N. Quaranta, Ceram. Inter. **29** (2003) 61-68
- [30] A. Karamanov, M. Aloisi, M. Pelino, J. Eur. Ceram. Soc. **25** (2005) 1531-1540
- [31] M. Ilic, C. Cheeseman, C. Sollars, J. Knight, Fuel **82** (2003) 331-336
- [32] V. Adell, C.R. Cheeseman, M. Ferraris, M. Salvo, F. Smeacetto, A.R. Boccaccini, Mater. Charact. **58** (2007) 980-988
- [33] A. Karamanov, M. Pelino, M. Salvo, I. Metekovits, J. Eur. Ceram. Soc. **23** (2003) 1609-1615
- [34] A. Mishulovich, J.L. Evanko, Ceramic International ash Symposium, Center for applied Energy Research, University of Kentucky, Paper 18 (2003)
- [35] M. Erol, S. Kúçúkbayrak, A. Ersoy Meriçboyu, Fuel **87** (2008) 1334-1340
- [36] Y.J. Park, S.O. Moon, J. Heo, Ceram. Inter. **29** (2003) 223-227.

BILJANA ANGJUSHEVA
EMILIJA FIDANCEVSKA
VOJO JOVANOVIĆ

Faculty of Technology and Metallurgy,
University "Ss. Cyril and Methodius",
Skopje, Republic of Macedonia

NAUČNI RAD

PROIZVODNJA KERAMIKE OD PEPELA UGLJA

Gusta keramika se dobija iz pepela iz REK Bitola u Republici Makedoniji. Predmet ovog istraživanja su četiri tipa pepela iz elektro filtera i jedan tip sa deponija sa česticama manjim od 0,063 mm. Konsolidacija se postiže pod pritiskom ($p = 133$ MPa) i sinterovanjem (na temperaturama 950, 1000, 1050 ili 1100 °C ibrinom zagrevanja od 3 ili 10 °C/min). Zgušnjavanje se postiže sinterovanjem tečnom fazom i reakcijom u čvrstom stanju, pri čemu se formira diopsid $(Ca(Mg,Al)(Si,Al)_2O_6)$. Keramika optimalnih karakteristika (poroznosti $2,96 \pm 0,5\%$, jačine savijanja 47 ± 2 MPa, čvrstoće 170 ± 5 MPa) je dobijena na 1100 °C brzinom zagrevanja od 10 °C/min.

Ključne reči: pepeo, keramika, sinterovanje, jačina savijanja, čvrstoća.